

Richness of cerebellar granule cell discharge properties predicted by computational modeling and confirmed experimentally



Masoli S.^{*1}, Tognolina M.^{*1}, Laforenza U.², Moccia F.³, D'Angelo E.^{1,4}

*Co-author

¹Department of Brain and Behavioral Sciences, University of Pavia, Pavia, Italy; ²Department of Molecular Medicine, University of Pavia, Pavia, Italy;

³Department of Biology and Biotechnology "L. Spallanzani", University of Pavia, Pavia, Italy; ⁴IRCCS Mondino Foundation, Pavia, Italy.



Human Brain Project

Abstract

The cerebellar granule cells (GrCs) are the most numerous neurons in the brain. Their highly packed distribution and misleading simple cytoarchitecture generated the idea of a limited spike generation mechanism. The typical regular spikes discharge, usually recorded for short periods of time (< 800ms) was the stepping stone for the simulation of realistic computational models. During short current injections (< 800ms), all GrC models conformed to the canonical firing pattern but, unexpectedly, prolonged current injections (2 sec) revealed a rich repertoire of adaptation properties, ranging from regular firing to different degree of firing adaptation. Patch-clamp recordings on parasagittal cerebellar slices from adult rats confirmed the modeling predictions on firing adaptation, while in a subset of experiments GrCs showed firing acceleration that was not found by the optimization technique. To simulate these GrCs, a TRPM4-like channel, known to mediate slow depolarizing currents, was linked to Calmodulin (Cam2C) concentration. This mechanism allowed to reproduce the accelerated state. Interestingly, the different firing properties impacted on synaptic transmission. When the mossy fiber bundle (MF) was stimulated at different frequencies (1-100 Hz), a range of filtering properties emerged, with adapting GrCs showing better transmission of high-frequency MF bursts over a background discharge than accelerating GrCs, suggesting a richness of encoding capabilities.

Materials and methods

Model: Automatic optimization of maximum ionic conductances was performed using the "Blue Brain Python Optimization Library" (BluePyOpt). The features were extracted from experimental traces of regular firing GrCs using the "Electrophys Feature Extraction Library" (EFeL). A single optimization took about 5 hours to be completed; the results were validated by evaluating spike generation and conduction. A model was discarded when (1) spike generation in the axonal initial segment failed, (2) spike conduction speed or spike amplitude in the ascending axon and parallel fibers was decremental, (3) spike frequency was different in soma and axon (± 1 spike/sec).

Patch clamp recordings: GrCs were recorded from the vermis central lobe of acute parasagittal cerebellar slices (230 μ m thick) from Wistar rats of either sex (p18-24) using a K-gluconate based intra-pipette solution and extracellular Krebs solution (2 mL/min, maintained at 32°C). Whole-cell data were acquired using a Multiclamp 700B amplifier and digitized with a Digidata 1440A/D converter (MolecularDevices).

Immunofluorescence: thin sections of the cerebellar vermis (20 μ m thick) were incubated with affinity pure primary antibodies and secondary antibodies (rabbit polyclonal anti-TRPM4, mouse monoclonal anti-Aquaporin 4 antibody [4/18] and goat anti-mouse IgG H&L, rhodamine red-X-conjugated affinity pure goat anti-rabbit IgG (H+L), respectively). Slices were examined with a TCS SP5 II confocal microscopy system equipped with a DM IRBE inverted microscope (LeicaMicrosystems) and visualized by LAS AF Lite software.

The complete material and method can be found on BioRxiv:

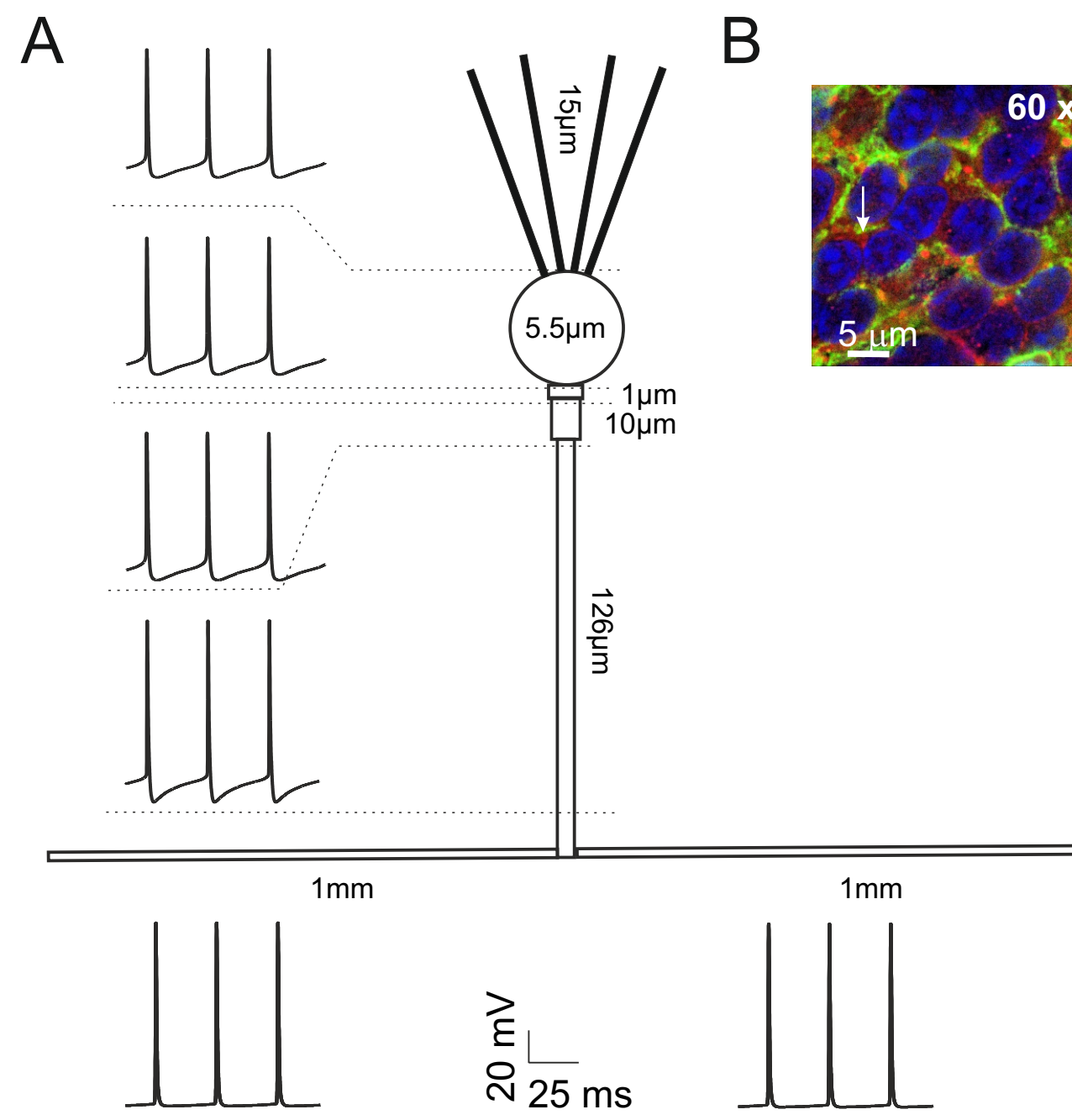
<https://www.biorxiv.org/content/10.1101/638247v1>

The models and experimental traces will be available, as a "dive paper", on the HBP collaboratory:

<https://collab.humanbrainproject.eu/#/collab/1655/nav/28538>

A. Schematic representation of GrC morphology (not in scale) and voltage traces generated in the different model sections during 10 pA current injection. The spike shape matches that reported by (Dover et al., 2016) and its timing and amplitude remain stable across the different sections.

B. Immunofluorescence image of a cerebellar slice stained with antibodies against TRPM4 (red), aquaporin-4 (green) and DAPI (blue). TRPM4 is expressed in the cell membrane surrounding the GrCs soma as well as in small grains in the cytoplasm (arrow).

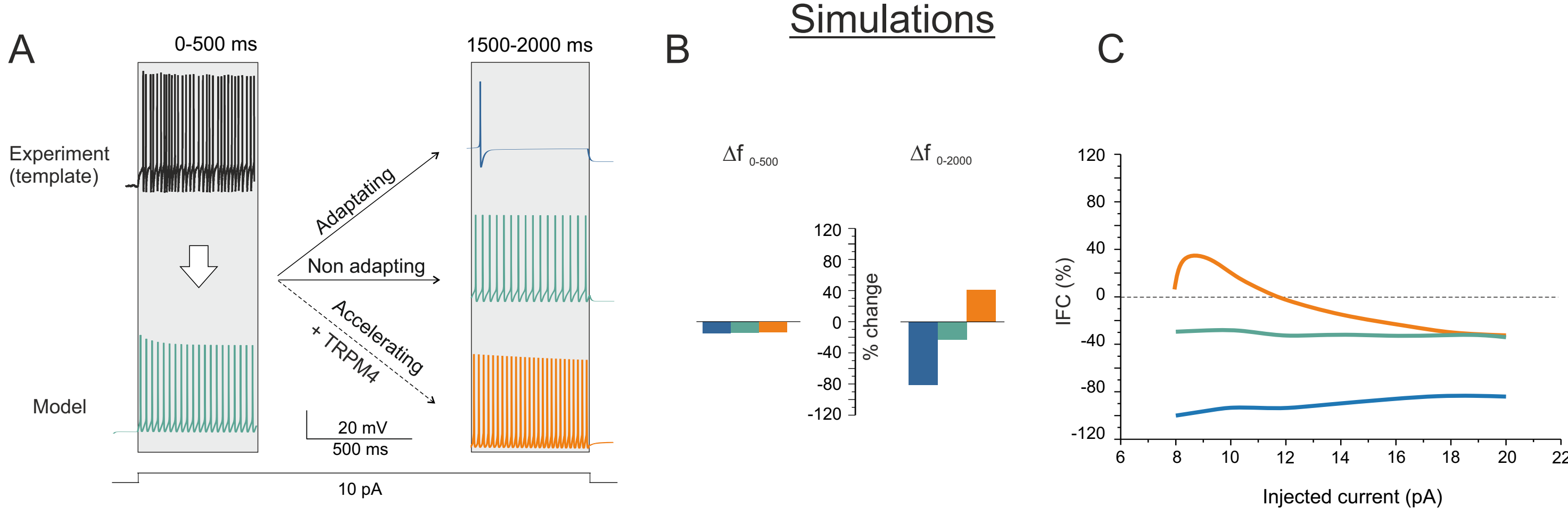


Conclusions

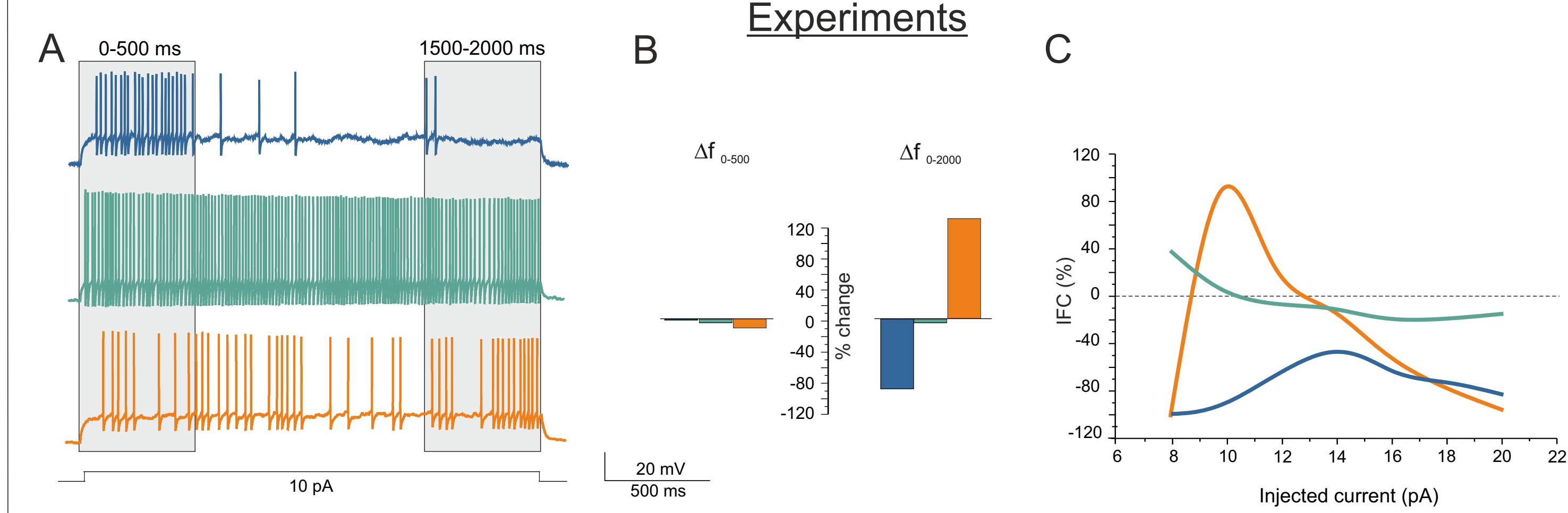
- The GrCs, with the same set of ionic channels, can provide quite distinct firing patterns;
- The different firing properties are reflected into differences in synaptic transmission;
- Optimization of maximum ionic conductances predicts:
 - 1) the different firing patterns;
 - 2) the nature of ionic channels regulation subtending adaptation and acceleration;
 - 3) the alignment of synaptic release probability with the firing patterns;

These results suggest that the richness of GrC adaptation and bursting properties may lead to generate information channels with differential filtering properties.

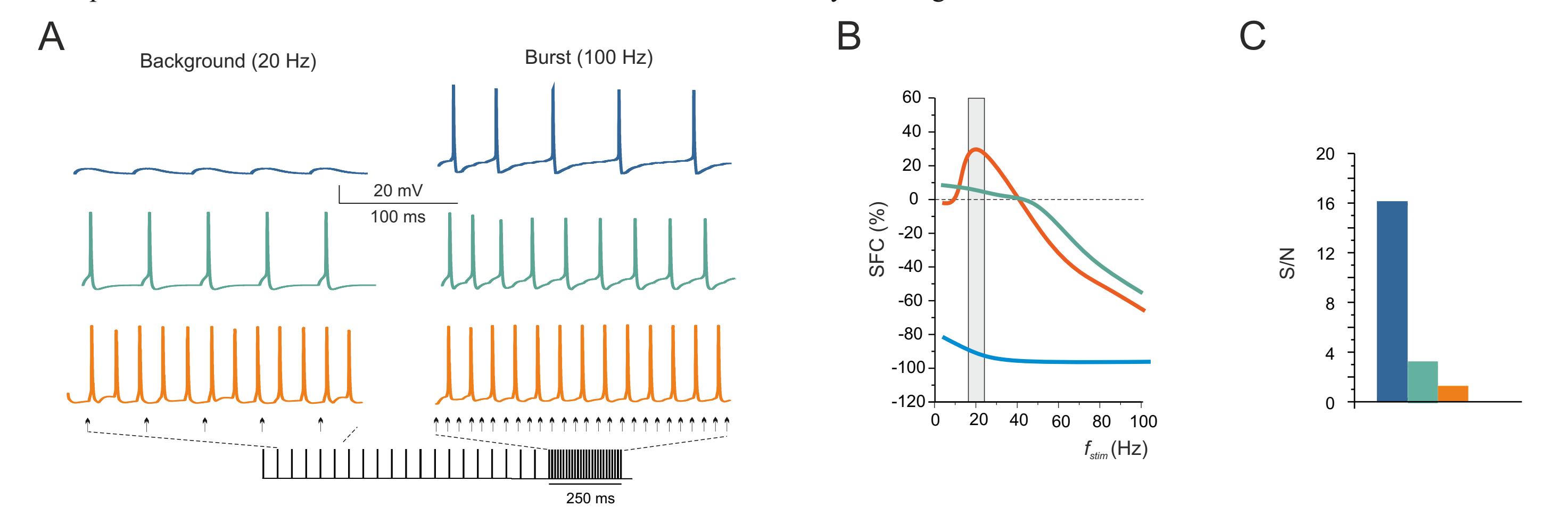
Modeling and experimental results



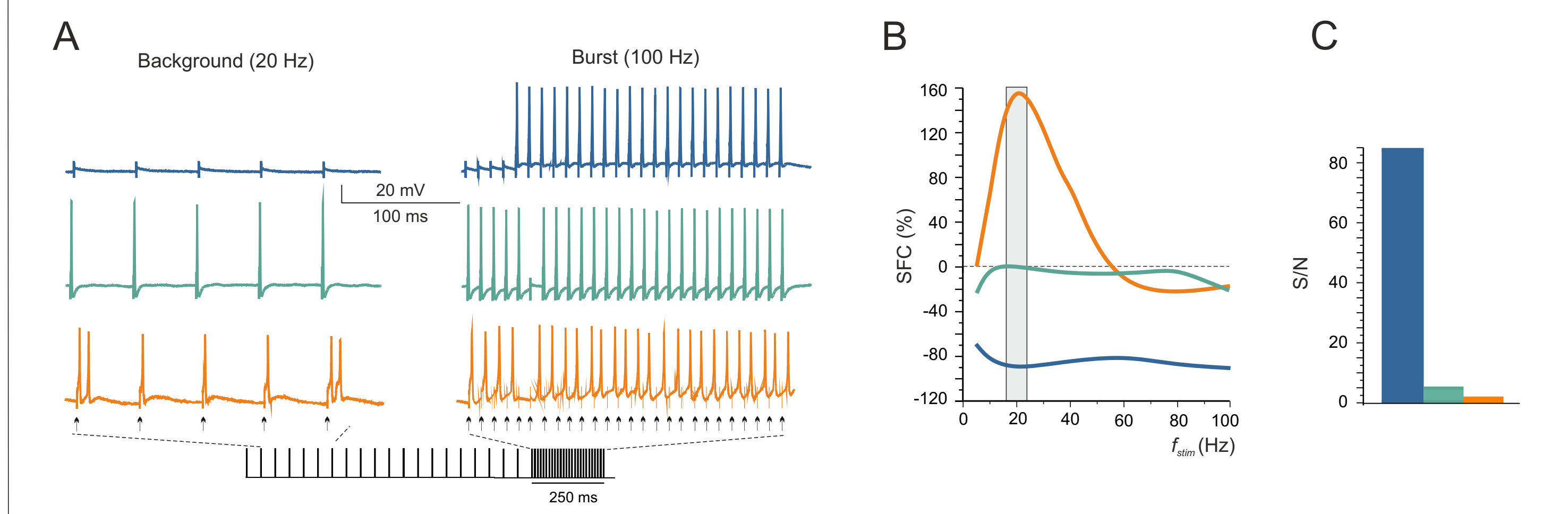
A. Voltage responses to 2000 ms - 10 pA current injection from the holding potential of -65 mV. The optimization run over the first 500 ms of discharge of a regular firing GrC (left) yields different discharge patterns at later times (1500-2000 ms, right). By adding a TRPM4/Ca²⁺/Calmodulin subcellular mechanisms the firing acceleration is reproduced. B. Histograms showing the spike frequency % changes after 500 ms and 2000 ms (Δf_{0-500} and Δf_{0-2000} , respectively). C. Plot of the intrinsic frequency change (IFC = $[(f_{final} - f_{initial})/f_{initial}] \%$) vs. injected current for the three GrC models. A positive peak is apparent in the accelerating GrC at 10 pA current injection, while negative IFC values prevail in the other GrCs. The same color codes are used consistently in the figures.



A. Voltage responses to 2000 ms - 10 pA current injection from the holding potential of -65 mV. Spike frequency initially remains stable in all the cells but it shows different trends thereafter. B. Histograms showing the spike frequency % changes after 500 ms and 2000 ms (Δf_{0-500} and Δf_{0-2000} , respectively). C. Plot of the intrinsic frequency change (IFC = $[(f_{final} - f_{initial})/f_{initial}] \%$) vs. injected current for the three GrCs. A positive peak is apparent in the accelerating GrC at 10 pA current injection, while negative IFC values prevail in the other GrCs. The same color codes are used consistently in the figures.

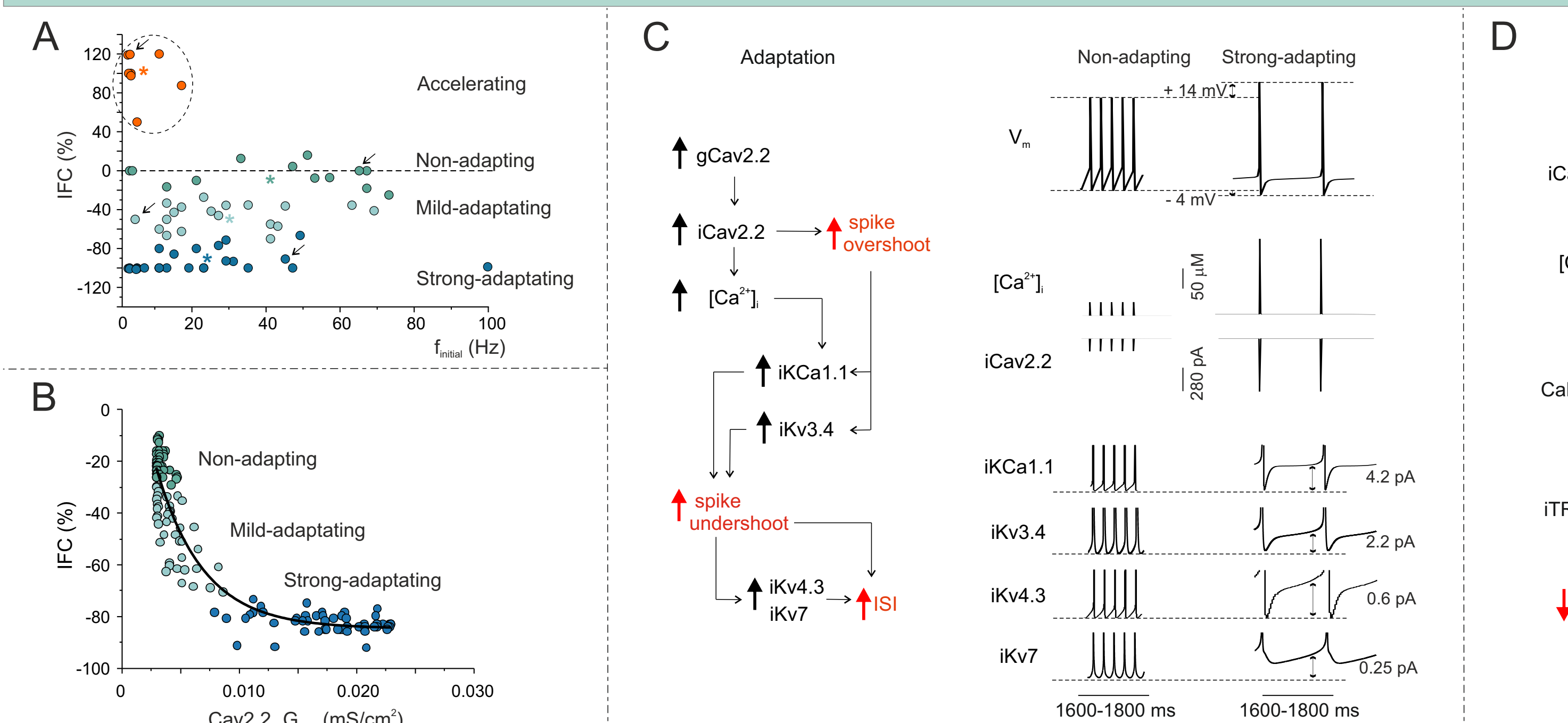


A. Voltage responses of GrC models to activation of the MF-GrC synapse (2 synapses, 1 sec continuous stimulation at 20 Hz followed by 250 ms at 100 Hz) from the holding potential of -65 mV. The p values are: $p=0.1$ for adapting GrC, $p=0.5$ for non-adapting and accelerating GrC. B. The synaptic frequency change ($SFC = [(f_{resp} - f_{stim})/f_{stim}] \%$) vs. stimulus frequency show a positive peak in the accelerating GrC model at 20 Hz background stimulation, while negative SFC values prevailed in the other GrC models. C. The signal-to-noise ratio, ($S/N = f_{resp}/f_{stim}$ at 100 Hz) is much higher in adapting GrC than in the others.



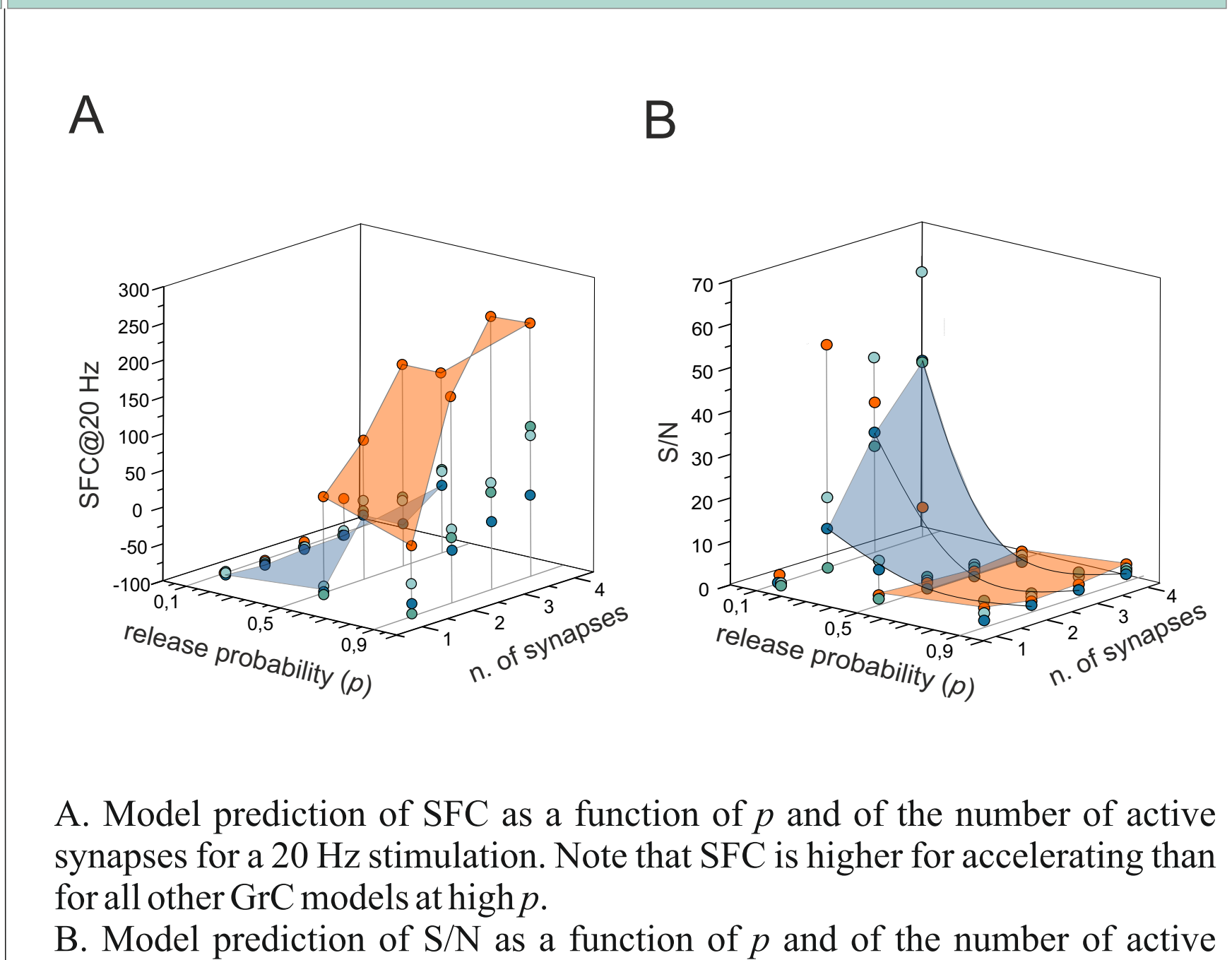
A. Voltage responses of exemplar GrCs to electrical stimulation of the MF bundle (1 sec continuous stimulation at 20 Hz followed by 250 ms at 100 Hz) from the holding potential of -65 mV. B. Plot of the SFC vs. stimulus frequency for the three GrCs shown in A. A positive peak is apparent in the accelerating GrC at 20 Hz background stimulation, while negative SFC values prevail in the other GrCs. C. S/N for the three GrCs in A-B. Note that S/N is much higher in adapting than in the other two GrCs.

Mechanisms generating firing adaptation and acceleration



A. An unbiased k-means cluster analysis applied to the experimental recordings ($n=63$ at 10 pA) identifies 4 statistically different data clusters ($p=3.7e-12$; Kruskal-Wallis test, * indicate the centroids of the 4 subpopulations). B. Distribution of IFC in GrC models with respect to the Cav2.2 maximum conductance (mS/cm^2), revealing a negative correlation ($R^2=0.88$, $n=150$, $p<10^{-10}$). Note the unbalance of Cav2.2 maximum conductance in favour of adapting GrCs. C. Scheme of the hypothetic chain of events leading to adaptation (left) and traces showing the voltage and intracellular Ca²⁺ concentration along with ionic currents in non-adapting and strong-adapting GrCs during 10 pA current injection at 1700 ms (right). Double arrows measure the difference between non-adapting and strong-adapting GrCs. D. Scheme of the hypothetic steps required for firing acceleration (left) and traces showing the voltage and intracellular Ca²⁺ concentration along with ionic currents and elements of the intracellular coupling mechanism in an accelerating GrCs during 10 pA current injection (right).

Synaptic responsiveness



A. Model prediction of SFC as a function of p and of the number of active synapses for a 20 Hz stimulation. Note that SFC is higher for accelerating than for all other GrC models at high p . B. Model prediction of S/N as a function of p and of the number of active synapses. Note that S/N is higher in strongly adapting GrC models at low p .

This project has received funding from the Horizon 2020 Framework Programme for Research and Innovation under the Specific Grant Agreement No. 720270 and 785907 (Human Brain Project SGA1 and SGA2).